



Quantum Turbulence: Part II .....6  
McIntosh's Kryo Kwiz .....13  
Schwenterly's Cold Cases.....19

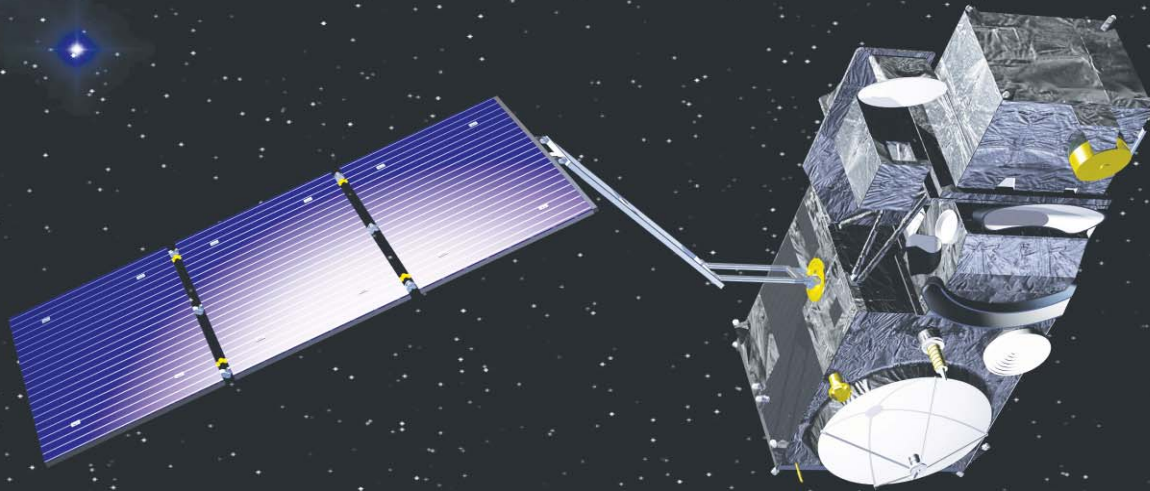
Birth and Rebirth of CSA .....26  
People, Companies in Cryogenics .....44  
Calendar .....45

# Cold Facts

The Magazine of the Cryogenic Society of America, Inc.

## INTERNATIONAL

Cryocoolers to Monitor Global  
Surface Temperatures  
From Space | 32



February 2014 | Volume 30 Number 1

# LN<sub>2</sub> Testing and Cleaning at NASA Ames' Transonic Wind Tunnel

by Victor Sloan, Victor Aviation Service, vic52@victor-aviation.com

The ability to identify and quantify changes in the microstructure of metal alloys is valuable in determining fatigue life and dependability of materials. For example, certain metals, after being Cryogenically Non-Destructive Tested (NDT) and treated, have shown large increases in their fatigue life. Similarly, improved life of components used in aerospace, vehicle, wind energy, turbine power plants and transmissions has also been documented and can reduce the total cost of ownership. However, the mechanisms of microstructure changes in alloys under various treatments, which cause them to behave differently, are not yet fully understood. Such changes are currently evaluated in a semi-quantitative manner either by visual inspection of microscopic images of the microstructure or by destructive examination of the test material.

The author's patent-pending cryogenic NDT and cryogenic transition detection processes using electromagnetic acoustical transmission (EMAT) or ultrasound transmission (UT) real-time recognition technology techniques quantitatively offer significant breakthroughs beyond existing techniques. They can measure the changes in microstructure and validate the initial assertion of improved fatigue life or material property characteristic changes under certain cryogenic NDT testing and treating processes. These innovations facilitate not only a better understanding of the effects of cryogenic treatment of these materials, but also their impact on residual stress, precipitation hardening and phase transformation of materials.

In order to evaluate residual stress in a metal alloy it is necessary to ensure that a complete phase transition has occurred to a stable crystalline structure and then treated to remove any unwanted residual stress. These patent pending cryogenic NDT and cryogenic

transition detection processes can provide significant advancements in the review of these changes and transformations that often occur in different manufacturing processes.

Under typical parts manufacturing conditions, temperature gradients can produce non-uniform dimensional and volume changes. When metal castings cool and solidify, compressive stresses develop in lower-volume areas, which cool first, and tensile stresses develop in areas of greater volume, which are last to cool. Shear stresses can develop between the different volume areas. This can happen even in large castings and machine parts of relatively uniform thickness. The surface cools first and the core last. In such cases, stresses develop as a result of the phase (volume) change between those layers that transform first and the center portion, which transforms last.

By further applying finite element analysis (FEA), a method for determining fatigue life prediction may also be determined along with dynamic stress and strain measurements. This method of cryogenic NDT testing for material property or residual stress component change becomes very effective as a quality control process for materials that will be applied, as it is a non-destructive testing process performed in real time.

In general, at least one new phase transition is formed that has different physical and chemical characteristics, and/or different microcrystalline structure from the pre-transformation phase. This happens over a time, de-

pendent on growth of the new phase from the formation (nucleation) and then growth of small regions of the new



NASA 11-by-11-foot Transonic Wind Tunnel Turbine Blades / Cryogenic Chamber. Photo: Victor Aviation Service

phase. The nucleation phase is dependent on the thermodynamic parameter of Gibbs free energy,  $G$ , which is a function of the enthalpy ( $H$ ), or the internal energy of the system. When the change in free energy is negative, the transformation will be driven spontaneously. This difference in free energy is dependent on the free energy difference between the new and old phase and due to the free energy at the boundary of the phases (surface free energy). The volume of free energy is related to the temperature ( $T$ ), surface free energy ( $\gamma$ ), latent heat of fusion ( $\Delta H_f$ ), equilibrium solidification temperature ( $T_m$ ):

$$\Delta G^* = \left( \frac{16\pi\gamma^3 T_m^2}{3\Delta H_f^2} \right) \frac{1}{(T_m - T)^2}$$

This results in a critical relationship of the volume of the new phase, providing it can pass through the threshold energy associated with formation of the critically small embryo volume of radius  $r^*$ .

$$r^* = \left( \frac{2\gamma T_m}{\Delta H_f} \right) \left( \frac{1}{T_m - T} \right)$$

## LN<sub>2</sub> Testing and Cleaning... Continued

Because free energy is temperature-dependent, the phase transitions are also temperature-dependent. A second temperature dependency is the clustering of atoms by short range diffusion in the formation of the nucleus. Hence the nucleation rate is temperature dependent and is suppressed at high temperatures due to a small activation driving force. The nucleation rate is also dependent on whether it forms within a nucleus (homogeneous) or at a surface (heterogeneous). This nucleation rate is also highly dependent on the addition of other atoms to the product, which is reflected in the necessary temperature of cooling to facilitate the equilibrium for nucleation.

These phase transitions may produce volume changes in the product and may lead to the introduction of microscopic strain, both of which have an impact on the physical characteristics and longevity of the product. Once nucleation has occurred, the growth of the embryo is dependent on exceeding the critical size where growth occurs spontaneously. Hence the degree of

phase change and the size of the phase particles will be both time- and temperature-dependent, and the amount of coarse or fine grains will vary as will the physical properties and stress in the product.

The cryogenic (NDT) and cryogenic transition detection methods are based on the effect of the microcrystalline structure on the transmission of ultrasound. These methods can be used to non-destructively evaluate the kinetics and completion of the time-temperature transformation between structural phases. Ultrasonic testing is based on the difference between the Young's moduli of the two phases at any given transformation temperature. Since the velocity of longitudinal sound waves is a function of the square root of the elastic constants, a change in velocity is expected during a typical transformation. Hence, the velocity should be somewhere between the two extremes with a mixture of the phases having a velocity in between.

Fortunately, voids do not affect ve-

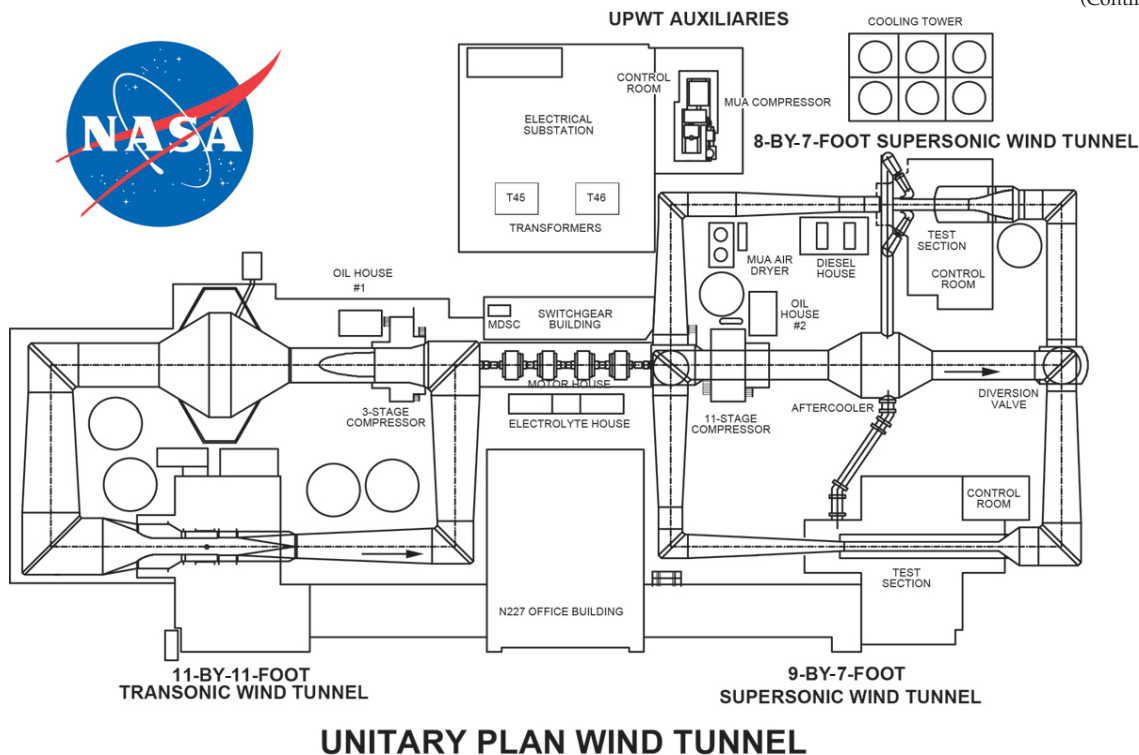
locity since the sound waves will pass only through the solid material. In addition to velocity changes, sound attenuation is also highly structure-sensitive, which may also give insight into the mechanism of the transformation. Unfortunately, since some scattering may occur at voids, this may be less reliable in determining the degree of transformation.

More specifically, the velocity of the longitudinal sound wave ( $V_l$ ) relates to the elastic constants as described by Hooke's law. The elastic constant relates to the linear stress and strain which are fundamentally functions of the thermodynamic state of the material and the interatomic binding forces in the microcrystalline lattice structure. The longitudinal velocity is related to the Young's modulus ( $E$ ), density ( $\rho$ ), and Poisson's ratio ( $\sigma$ ) by

$$V_l = \left[ \frac{E}{\rho} \frac{1 - \sigma}{(1 + \sigma)(1 - 2\sigma)} \right]^{1/2}$$

In order to utilize this to non-

(Continued on page 40)



destructively assess the transformation within an alloy, sound waves are assessed for transit time through a structure. This time (T) will be related to longitudinal velocity (V) and path length (L) by

$$\tau = \frac{L}{V}$$

Since changes in length will be small during the phase transformation, changes in transit time will reflect changes in the properties of the product and the progress of transformation. Hence the use of ultrasonic transit time measurements can allow the non-destructive assessment of the optimal time and temperature treatment while reducing excessive treatment and the need for multiple treatment cycles, both of which will reduce the desirable mechanical properties.

By performing real-time ultrasound testing procedures using electromagnetic acoustic transmission (EMAT) or conventional ultrasonic (UT) while performing real-time cryogenic NDT testing, any changes in a material's velocity and amplitude can be documented. The time and temperature is recorded upon any change in velocity or amplitude, and phase transformation detection of the start and completion of transition and can be documented. These

cryogenic NDT testing processes become quite valuable in establishing quality control procedures for materials manufacturers and as an incoming materials inspection process.

Another benefit of the cryogenic NDT testing and cryogenic transition detection processes are that not only can these processes detect residual stress, precipitation hardening or incomplete phase transitions, they can relieve residual stress and complete any incomplete phase transitions simultaneously. The use of these cryogenic NDT testing and treating processes enables manufacturers and incoming material inspectors to identify material properties that they had never been able to non-destructively detect. Cryogenic NDT testing also provides for quantitative testing results and validation of cryogenic stress relieving processes performed.

To demonstrate the capabilities of cryogenic NDT, a case study test was performed on 2014 aluminum Transonic Wind Tunnel Turbine Blades that had been removed from service from the NASA Ames Research 11-x-11-foot



NASA Ames Research Center Unitary Plan Wind Tunnel Complex (UPWT) - Moffett Field, California. Photo: NASA

Unitary Plan Wind Tunnel (UPWT). Victor Aviation Service, Inc. is a NASA approved contractor for the UPWT.

The 11-x-11-foot Transonic Wind Tunnel Facility is part of the Unitary Plan Wind Tunnel complex at NASA's Ames Research Center at Moffett Field CA. Several generations of commercial and military aircraft and NASA space vehicles, including models of the space shuttle and Mercury, Gemini and Apollo capsules, have been designed and tested at the UPWT.

NASA's 11-x-11-foot wind tunnel design is a closed-return, variable-density tunnel with a fixed geometry, ventilated test section with a flexible wall nozzle. It is one of three separate test sections powered by a common drive system. The aluminum turbine blades are used in a three-stage, axial-flow compressor powered by four wound rotors with variable-speed induction motors, producing airflow up to 1.5 Mach. Interchangeability of models across a wide range of conditions.



Dual Polarized EMAT Testing / NASA 11-by-11-foot Transonic Unitary Wind Tunnel Turbine Blade. Photo: Victor Aviation Service

X-ray Diffraction Stress Measurements - Cryogenic (NDT)	
Virgin Material Coupon A	Coupon C after Cryogenic NDT Testing
0 Degree Reference X-Ray Sensor Position Sigma (x) -125 MPa Tau (xy) 7MPa FWHM 1.78	0 Degree Reference X-Ray Sensor Position Sigma (x) -64 MPa Tau (xy) 14 MPa FWHM 1.71
90 Degree Reference X-Ray Sensor Position Sigma (x) -103 MPa Tau (xy) 12MPa FWHM 1.83	90 Degree Reference X-Ray Sensor Position Sigma (x) -46 MPa Tau (xy) 49 MPa FWHM 1.70

X-ray Diffraction Stress Measurements - Plastic Shot Peening	
Coupon 54 Before Plastic Shot Cleaning	Coupon 54 after Plastic Shot Cleaning
0 Degree Reference X-Ray Sensor Position Sigma (x) -83 MPa Tau (xy) -6 MPa FWHM 1.72	0 Degree Reference X-Ray Sensor Position Sigma (x) -227 MPa Tau (xy) -1 MPa FWHM 2.07
90 Degree Reference X-Ray Sensor Position Sigma (x) -77 MPa Tau (xy) -46MPa FWHM 1.73	90 Degree Reference X-Ray Sensor Position Sigma (x) -219 MPa Tau (xy) -19 MPa FWHM 2.17

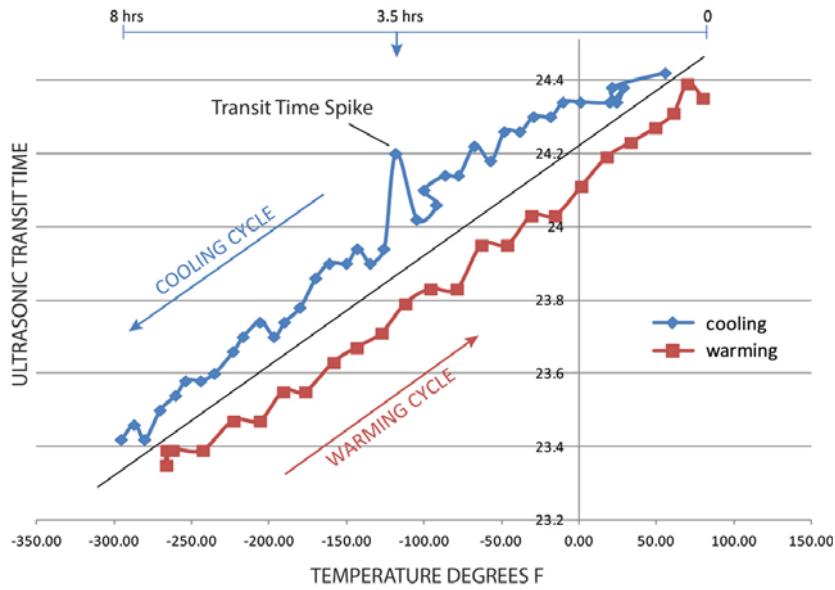


**(Figure A) Hysteresis Graph - EMAT Ultrasonic Transit Time vs. Temperature in Degrees F. / NASA Turbine Blade. Image: Victor Aviation Service**

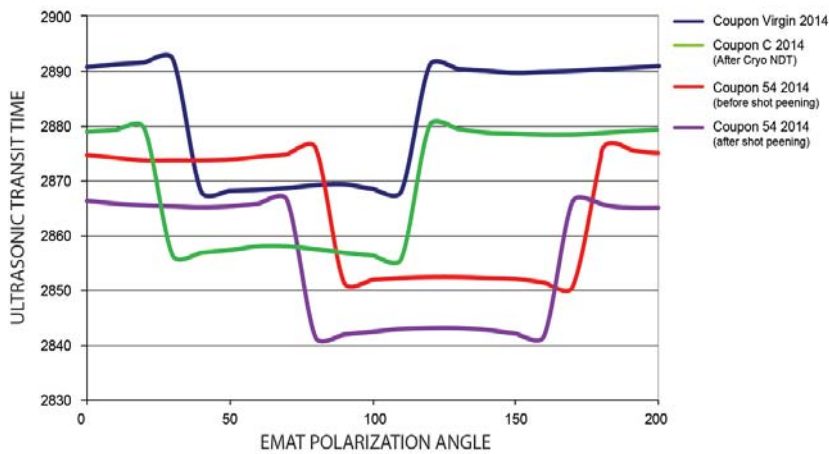


**(Figure B) Birefringence Stress Test - Ultrasonic Transit Time vs. Polarization Angle - 2014 Aluminum Coupons. Image: Victor Aviation Service**

The Transonic Wind Tunnel Turbine Blades were cryogenic NDT tested from a room temperature of 74 °F to -310 °F to 74 °F while real time ultrasonically monitored using an EMAT sensor system developed by Victor Aviation Service, Inc. For test comparison purposes, 2014 aluminum etched and 180 grit sanded coupons were also included in the test processes.

An example hysteresis graph (Figure A) illustrates a transit time vs. tem-

perature hysteresis plot for the cooling and re-heating stages of the turbine blades while in a cryogenic liquid nitrogen atmosphere chamber over a 16-hour cooling and heating cycle. This hysteresis chart plots the ultrasonic transit time of sound being transmitted through the thickness of the aluminum turbine blade while being cryogenic NDT tested in real time.

During the cooling stage at approximately -123 °F degrees and 3.5 hours



**Pulstec X-360n X-Ray Diffraction Testing / NASA Turbine Blade - 0 Degree Position. Photo: Victor Aviation Service**



**Pulstec X-360n X-Ray Diffraction - 90 degree position. Photo: Victor Aviation Service**

into the ramp down of the cryogenic NDT test process, you will note a transit time spike in the hysteresis curve. This hysteresis curve information indicates that a stress component change has been detected in the turbine blade. As the cryogenic NDT process continued the cycle from -123 °F to -310 °F and reheated back to 74 °F, you will note that on the heating cycle that the transit time spike has disappeared at -123 °F, indicating that the stress component previously identified at -123 °F was stabilized and the slope of the hysteresis curve was uninterrupted.

Prior to the cryogenic NDT testing, X-ray diffraction was performed at Victor Aviation Service, Inc. on the aluminum 2014-C etched and 180 grit sanded coupon using a Pulstec X360n X-ray diffraction sensor. The Sigma (x) MPa residual stress and Tau (xy) MPa shear stress was tested. X-ray stress measurements were taken at the 0° surface sample Z axis and also at the 90° surface sample Z axis. Following testing these same X-ray stress tests were repeated. X-ray diffraction measures the change in the atomic lattice structure of the crystal structure of the material. You will note that the residual

(Continued on page 42)

stress comparisons indicated that the atomic lattice structure had changed following testing. (See Figures 1-4.)

A room temperature 74°F birefringence stress test was also performed prior to and following testing using a dual polarized shear wave EMAT sensor on the turbine blades. This process measures the ultrasonic transit time of the 2014 aluminum measured as a comparison to the fast and slow transit time axis of the turbine blade. The birefringence test results also documented the change in stress condition at various points on the turbine blade when comparing the before and after NDT process ultrasonic birefringence data. (See Figure B on page 41.)

Following the cryogenic NDT testing phase, the 2014-54 aluminum coupon was shot peened using plastic cleaning media Type II -20/30- Mil in accordance with Military Specification Mil-P-85891 in a plastic media shot peening chamber at Victor Aviation Service, Inc. A calibrated Electronics Inc. Almen gauge and aero aluminum Almen strips were used to determine and verify the intensity of the shot peen cleaning process and validated with X-ray diffraction analysis. X-ray diffraction was again performed on the 2014-54 aluminum coupon indicating that the surface residual stress increased. (See Figures 5-8.)

### Conclusion

It was noted that the 2014-C etched aluminum coupon was residual stress relieved using cryogenic NDT testing due to the reduction in observed MPa stress as measured before and after testing. This was also confirmed by through-thickness EMAT averaged birefringence transit time test comparisons. The random surface MPa stress measurements of the turbine blades and coupons also became more uniform for near surface residual stress and validated by X-ray diffraction MPa stress data.

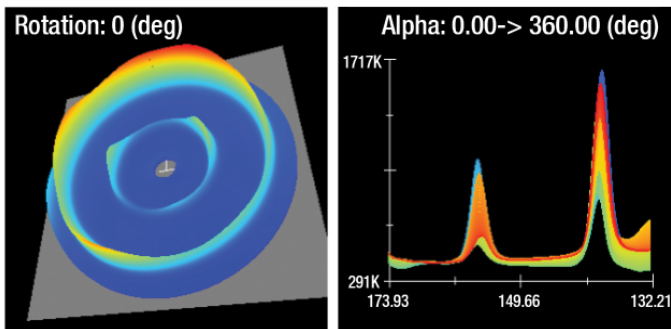
As a result of the two processes applied by cryogenic NDT testing and plastic media shot cleaning of the 2014 aluminum coupons, the surface residual compressive stress increased. These processes provide for a higher resistance to contact surface fatigue failure, corrosion fatigue and stress corrosion cracking.

The cryogenic NDT stress relieving process of the 2014 aluminum prior to plastic media shot cleaning created a more uniform finished surface residual compressive stress. It is the professional opinion of Victor Aviation Service, Inc. that the applied surface compressive stress induced from plastic shot peen cleaning, coupled with a more uniform material residual stress after testing,

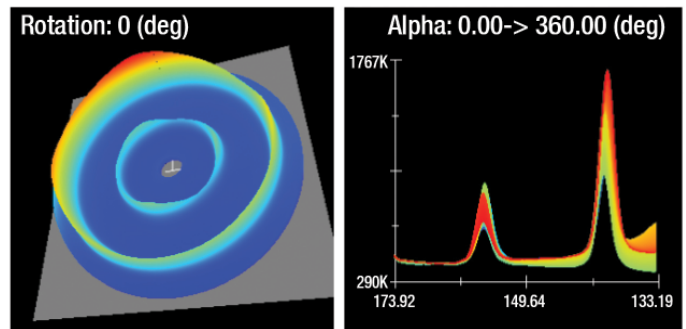
can provide a better equilibrium of stress components, reduced maintenance and improved material stability.

### References

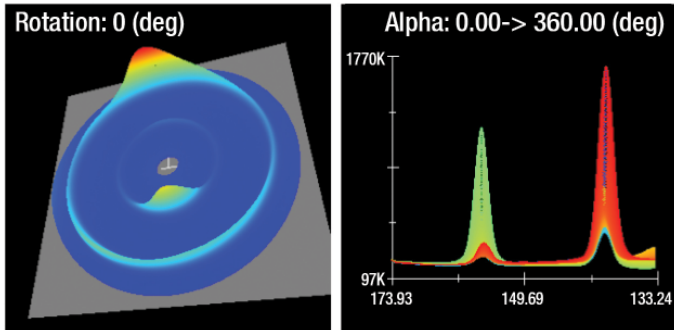
1. Barron, R.F., Cryogenic Heat Transfer, Edwards Brothers, Ann Arbor, 1999.
2. Jordine, A., Increased Life of Carburized Race Car Gears by Cryogenic Treatment Proc., IMMA Conf., 1995, 107-111.
3. Ray, B.C., S.T. Hasan, and D.W. Clegg, Effects of Thermal Shock on Modulus of Thermally and Cryogenically Conditioned Kevlar/Polyester Composites, J. Of Materials Science Letters, Vol 22, 2003, 203-204.
4. Sahoo, B.N., Effect of Cryogenic Treatment of Cemented Carbide Inserts on Properties & Performance Evaluation in Machining of Stainless Steel, Department of Mechanical Engineering National Institute of Technology, 2011.
5. Callister, W, Rethwish, D, Fundamentals of Materials Science and Engineering, Third Edition, 2008.



**Debye Ring (3D)** **Profile**  
**Figure 1. Virgin 2014 aluminum coupon - 0 degree. Sigma (x): -125 MPa; Tau (xy): 7 MPa; FWHM: 1.78 deg.**



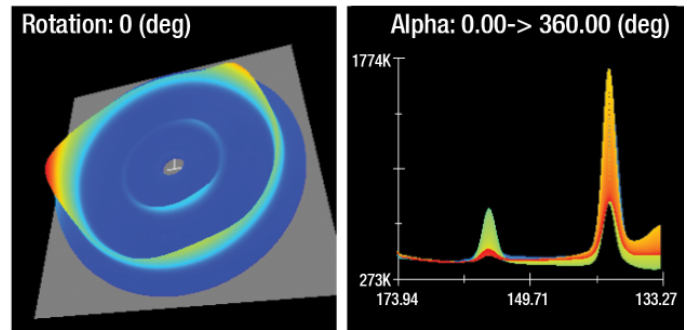
**Debye Ring (3D)** **Profile**  
**Figure 2. Virgin 2014 aluminum coupon - 90 degree. Sigma (x): -103 MPa; Tau (xy): 12 MPa; FWHM: 1.83 deg.**



**Debye Ring (3D)**

**Profile**

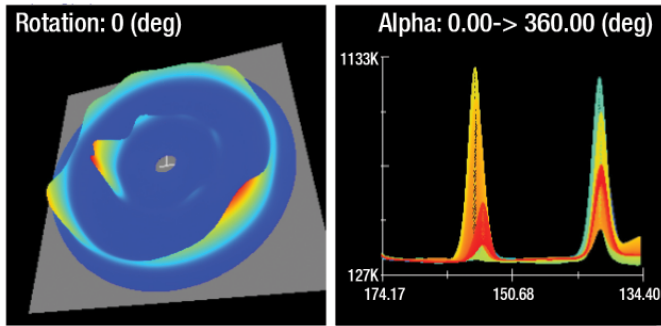
Figure 3. 2014 Aluminum coupon after cryogenic NDT - 0 degree. Sigma (x): -64 MPa; Tau (xy): 14 MPa; FWHM: 1.71 deg.



**Debye Ring (3D)**

**Profile**

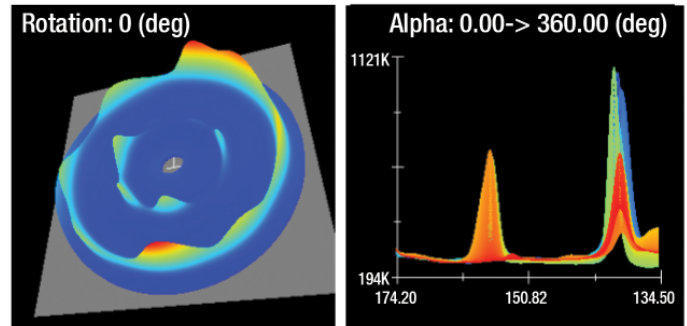
Figure 4. 2014 Aluminum coupon after cryogenic NDT - 90 degree. Sigma (x): -46 MPa; Tau (xy): 49 MPa; FWHM: 1.70 deg.



**Debye Ring (3D)**

**Profile**

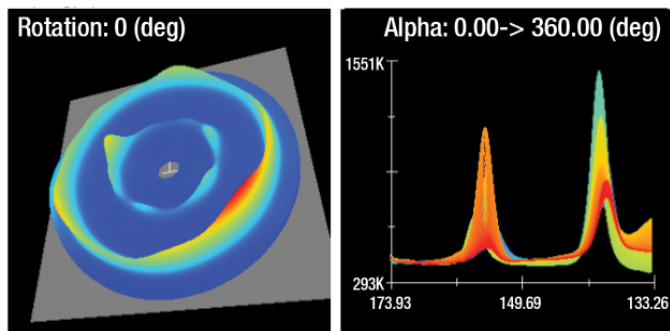
Figure 5. 2014 Aluminum coupon before plastic shot cleaning - 0 degree. Sigma (x): -83 MPa; Tau (xy): -6 MPa; FWHM: 1.72 deg.



**Debye Ring (3D)**

**Profile**

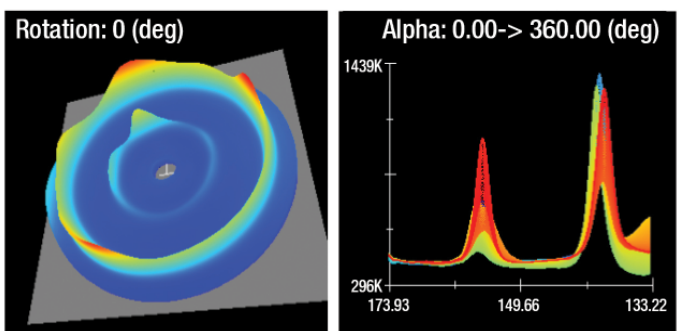
Figure 6. 2014 Aluminum coupon before plastic shot cleaning - 90 degree. Sigma (x): -77 MPa; Tau (xy): -46 MPa; FWHM: 1.73 deg.



**Debye Ring (3D)**

**Profile**

Figure 7. 2014 aluminum coupon after plastic shot cleaning - 0 degree. Sigma (x): -219 MPa; Tau (xy) -19 MPa; FWHM: 2.17 deg.



**Debye Ring (3D)**

**Profile**

Figure 8. 2014 aluminum coupon after plastic shot cleaning - 90 degree. Sigma (x): -227 MPa; Tau (xy): -1 MPa; FWHM: 2.07 deg.

**Debye Ring (3D)**—The circular patterns are called Debye rings. They are produced by the diffraction of X-rays from the crystal lattice of the specimen as determined by Bragg's law. The angles of diffraction and the size of the resulting Debye rings are characteristic of the metal being examined.

**FWHM**—Full Width at Half Maximum of Diffraction. Crystallite size is reflected in the broadening of a particu-

lar peak in a diffraction pattern associated with a particular planer reflection from within the crystal unit cell. It is inversely related to the FWHM of an individual peak. The more narrow the peak, the larger the crystallite size.

**Profile**—Diffraction peak position, intensity and Bragg's angle. 